

First-principles investigations on the structural, electronic and magnetic properties of Cr-doped $(\text{ZnTe})_{12}$ clusters

Hong-Xia Chen*

College of Physical Science and Electronic Techniques, Yancheng Teachers University,
Yancheng 224002, China

Received 5 October 2010; Accepted (in revised version) 25 October 2010

Published Online 28 March 2011

Abstract. We have studied the structural, electronic and magnetic properties of $(\text{ZnTe})_{12}$ clusters doped with one (monodoped) and two (bidoped) Cr atoms in terms of a first-principles method. Substitutional, exohedral, and endohedral doping are considered. The exohedral isomer is found to be most favorable in energy for monodoped clusters, while the endohedral isomer is found to be most favorable for bidoped ones. The magnetic coupling between the Cr atoms is mainly governed by the competition between direct Cr-Cr antiferromagnetic (AFM) interaction and the ferromagnetic (FM) interaction between two Cr atoms via Te atom due to strong p-d hybridization. Calculations indicate that the substitutional bidoped $(\text{ZnTe})_{12}$ clusters favor the FM state, which has potential applications in nanoscale quantum devices.

PACS: 71.15.Mb, 73.61.Ga, 75.50.Pp

Key words: diluted magnetic semiconductor, clusters, density functional theory

1 Introduction

The discovery of ferromagnetism in Mn-doped GaAs with a Curie temperature of 110K has created an intense interest in the study of dilute magnetic semiconductors (DMS) [1]. Studies of these systems are driven not only by the academic interest in understanding the origin of ferromagnetism but also by the potential applications. ZnTe is a direct wide band-gap (2.26 eV) II-VI semiconductor. Among other II-VI DMS, Cr-doped ZnTe has also been studied both experimentally and theoretically. For instance, Saito *et al.* [2] reported the occurrence of high Curie temperature ferromagnetism in epitaxially grown thin films of Cr-doped ZnTe. Pekarek *et al.* [3] have reported room temperature ferromagnetism in bulk Cr-doped ZnTe

*Corresponding author. Email address: chenhongxia1@sina.com (H. X. Chen)

crystal. Theoretical calculations have also revealed the possibilities of achieving strong FM order in Cr-doped bulk ZnTe. Sato *et al.* [4] reported from KKR-CPA studies that ferromagnetism in Cr-doped bulk ZnTe is more stable than other TM (Mn, Fe, and Co) doped cases.

Compared with bulk and film, cluster usually displays some unique properties due to its special geometry and the quantum confinement effect, which hold promise for advanced nanodevice applications [5–7]. With the recent emergence of nanoscience and nanotechnology, doping of clusters and nanoparticles has also attracted a great deal of attention because of their prospects in technological applications [8–11]. The pristine ZnTe clusters have been studied theoretically [12, 13]. Among these cage-like ZnTe structures, the $(\text{ZnTe})_{12}$ is the smallest cage structure with the highest possible symmetry (octahedral), which can be taken as a good candidate for the investigation of Cr-doped ZnTe clusters. Previous works have been performed on the $(\text{ZnO})_{12}$, $(\text{GaAs})_{12}$, and $(\text{CdS})_{12}$ clusters doped with TM atoms [14–16]. Recently, Yadav *et al.* [17] have reported that both the short-ranged FM and AFM coupling could exist in the Cr-doped $(\text{ZnTe})_{12}$ clusters, depending on the Cr-Cr distance and the local environment of Cr atoms. But they only considered the substitutional doping. As we know, Cr atom can interact with the host cluster in three possible ways, (a) replace the atom from the host cluster (substitutional); (b) occupy the center of the cage formed by the host cluster (endohedral); (c) absorbed on the surface of the host cluster (exohedral). In this paper, we present a systematical theoretical investigation on the geometry, electronic and magnetic properties of $(\text{ZnTe})_{12}$ clusters doped with one or two Cr atoms. The exohedral isomer is found to be most favorable in energy for monodoped clusters, while the endohedral isomer is found to be most favorable for bidoped ones. The magnetic coupling between the Cr atoms is mainly governed by the competition between direct Cr-Cr AFM interaction and the FM interaction between two Cr atoms via Te atom due to strong *p-d* hybridization.

2 Theoretical method and computational details

The calculations are performed using spin-polarized density functional theory (DFT). All electrons treatment and double numerical basis set including *d*-polarization functions (DND) are chosen. The Direct Inversion in an Iterative Subspace (DIIS) approach is used to speed up Self-consistent field (SCF) convergence. We also apply thermal smearing to the orbital occupation to speed it up. For the accurate calculations, we have chosen an octupole scheme for the multipolar expansion of the charge density and Coulomb potential. The exchange-correlation interaction is treated by generalized gradient approximation (GGA) with the functional parameterized by Perdew-Burke-Ernzerhof correction (PBE) [18]. SCF calculations are done with a convergence criterion of 10^{-6} hartree on the total energy. All structures are fully optimized without any symmetry constraint with a convergence criterion of 0.002 hartree/Å for the forces and 0.005 Å for the displacement. Mulliken population analysis [19] is performed to determine the charge transfer and magnetic moment on each atomic site.

As is well known in the cluster, the orbital magnetic moment is quenched and the magnetic moment comes exclusively from the spin of the electrons [20]. Throughout this work we do

not consider the relativistic effects, e.g., the spin-orbital coupling. As a result, the magnetic moments provided in this study reflect the spin-only values. For the Cr₂ dimer, at the level of PBE/DND its ground state is an AFM configuration. The molecule has a bond length of 2.19 Å, and binding energy of -1.25 eV compared to the experimental values of 1.68 Å and -1.42 eV, respectively [21]. In addition, the previous studies [14–16] have indicated that the main conclusions on the structural stability, the electronic and magnetic properties of the doped semiconductor clusters are reliable at GGA/PBE level. Thus, we believe that our computational scheme is appropriate for describing the properties of the Cr atoms doped (ZnTe)₁₂ cluster.

Commonly, the thermodynamic stability of a cluster is determined by its binding energy, which is defined as

$$E_b = \left(E_{tot} - \frac{\sum_i E_{atom}^i}{\sum_i n_i} \right),$$

where E_{tot} , E_{atom}^i and n_i are the total energy of the cluster, the energy, and the number of the i -th isolated atom, respectively. Furthermore, the fragmentation energy is introduced to indicate the stability of the cluster, especially for comparison between various isomers with different chemical composition. In general, for a fragmentation channel A→B+C, the fragmentation energy can be defined as $\Delta E = E_B + E_C - E_A$, where E_B , E_C and E_A are the total energies of clusters B, C, and A, respectively.

3 Results and discussion

3.1 Pristine (ZnTe)₁₂ clusters

We first consider the pristine (ZnTe)₁₂ cluster, which is found to be highly stable at a fullerene-like structure (T_h symmetry) with eight hexagons and six isolated squares. There are two un-equivalent Zn-Te bonds: the Zn-Te bond inside the four-member rings has a length of 2.672 Å, while that between the four-member rings has a length of 2.603 Å. The noticeable cavity in the structure, which corresponds to an utmost interatomic distance of 7.200 Å between Zn atoms or 8.807 Å between Te atoms, provides a possibility for endohedral doping. The large HOMO-LUMO gap of 2.87 eV indicates the semiconductor nature as well as high stability character of the cluster. Our spin-polarized calculations indicate that the pristine (ZnTe)₁₂ cluster is a closed shell system without any local atomic magnetic moment.

3.2 Monodoped (ZnTe)₁₂ clusters

3.2.1 Geometrical structure

The ground state structure is considered for five different kinds of monodoping structures. (a) A1: a Cr atom substitutes one Zn atom. (b) A2: a Cr atom is endohedral into the center of the cage. (c) A3: a Cr atom is initially placed at the hollow site of a Zn and two Te atoms within a square surface. After geometry optimization, the Cr atom occupies original Zn position and

pushes the Zn atom away. (d) A4: a Cr atom bridges over a Zn-Te bond that connects two squares. After geometry optimization, the Cr atom connects two squares by forming Zn-Cr and Cr-Te bonds. (e) A5: a Cr atom bridges over a Zn-Te bond of square. After geometry optimization, the Cr atom connects two neighboring Te atoms. The fully optimized structures are shown in Fig. 1(a). Apart from the formation of new bonds due to the inclusion of a Cr atom, the other bond lengths in these clusters are more or less similar to those in the pristine $(\text{ZnTe})_{12}$ cage. We also note that the substitutional doped isomer A1 has similar geometry with the pristine $(\text{ZnTe})_{12}$ cluster, though the Cr-Te bond is a little larger than Zn-Te bond.

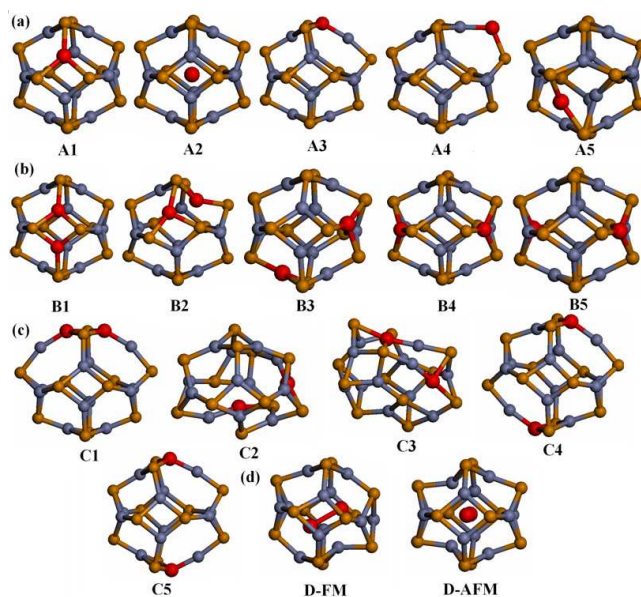


Figure 1: Fully optimized structures of various isomers of doped $(\text{ZnTe})_{12}$ clusters. Blue ball, Zn atom; brown ball, Te atom; red ball, Cr atom.

3.2.2 Energetic and stability

In order to explore the stability of the doped clusters, we calculated the binding energy, HOMO-LUMO gap, and the fragmentation energy. The results are presented in Table 1. For the isomers A2-A5 with the same chemical composition, the most stable isomer is A5, indicating that exohedral isomer is more favorable than endohedral one. Similar behavior was found for the Mn-doped $(\text{ZnO})_{12}$ and Cr-doped $(\text{CdS})_{12}$ cage [14, 16]. While for the Mn-doped $(\text{GaAs})_{12}$ cage, the endohedral isomer is more favorable than exohedral one [15]. The HOMO-LUMO gaps of all doped isomers are smaller than that of the pristine $(\text{ZnTe})_{12}$ cluster (2.87 eV) due to the newly formed hybridized states.

The fragmentation energies are calculated by two different channels. One is "Cr-doped cluster \rightarrow $(\text{ZnTe})_{12}$ cluster + an isolated Cr atom" denoted as ΔE_1 . Larger positive value represents that the Cr-doped isomer is more stable. For the substitution case, the total energy of the "Cr-doped" cluster is set as sum of the total energies of A1 and Zn atom. The other

Table 1: The binding energy (E_b , in eV/atom), HOMO-LUMO gap (in eV), fragmentation energies (ΔE_1 and ΔE_2 , in eV), local charge (Q_{Cr} , in a.u.), magnetic moment (μ_{Cr} , in μ_B) of Cr atom, and total magnetic moment (μ_{tot} , in μ_B) of Cr-doped $(ZnTe)_{12}$ clusters. The magnetic moments contributed by the nearest neighboring Zn (μ_{Zn} , in μ_B) and Te atoms (μ_{Te} , in μ_B) are also shown.

Isomers	E_b	Gap	ΔE_1	ΔE_2	μ_{Zn}	μ_{Te}	Q_{Cr}	μ_{Cr}				μ_{tot}
								4s	4p	3d	total	
A1	-2.211	0.84	1.44	0.00	-	-0.34	0.30	0.17	0.11	3.99	4.27	4.00
A2	-2.127	1.19	1.54	0.10	0.24	0.13	-0.07	0.67	0.09	4.83	5.58	6.00
A3	-2.120	0.84	1.37	-0.07	-0.15	-0.16	0.19	0.17	0.11	4.07	4.35	4.00
A4	-2.097	0.52	0.78	-0.66	-0.17	-0.18	0.20	0.22	0.03	4.42	4.66	4.00
A5	-2.138	0.94	1.81	0.37	-0.16	-0.04	0.12	0.14	0.14	4.08	4.36	4.00

is "Cr-doped cluster \rightarrow isomer A1 + an isolated Zn atom" denoted as ΔE_2 . Larger positive value represents that the Cr-doped isomer is more stable. As listed in Table 1, the positive values of ΔE_1 for all cases imply that the pristine $(ZnTe)_{12}$ cluster can easily accommodate a Cr atom. The positive values of ΔE_2 suggest that the exohedral and endohedral doping are more stable than substitutional doping isomer. For example, ΔE_2 of isomer A5 is 0.37 eV. This indicated that isomer A5 is slightly more favorable than the complex of substitution isomer A1 and an isolated Zn atom. Previous calculations have indicated that the hollow cage structure composed of four-member and six-member rings has relatively lower energy [12, 13]. From Fig. 1(a), we can see that the Cr atom connected with the two neighboring Te atoms in isomer A5, which forming two six-member rings. It tells us that Cr atom prefer to absorbing on the surface of the host cluster when they are doped into the cluster.

3.2.3 Electronic and magnetic properties

Based on the optimized geometries, the magnetic properties of all doped clusters are computed and the results are presented in Table 1. Monodoped isomers show interesting magnetic properties. All isomers have total magnetic moments $4\mu_B$ except A2 whose total magnetic moment is $6\mu_B$. The magnetic moment is mainly contributed by the 3d component of Cr atom, while the 4s and 4p orbital also have certain contributions. Due to the hybridization interaction, a small magnetic moment is induced in nearest neighboring Te and Zn atoms. From all the above, we can conclude that the magnetic moment of Cr-doped clusters is dependent on the local environment of the Cr atom. The same as Similar behavior was observed for the Cr-doped $(CdS)_{12}$ clusters [16].

It is well-known that the local magnetic properties of a TM impurity strongly depend on the local environment. The decreasing ordering of local magnetic moment of Cr is A2, A4, A5, A3, and A1. The local magnetic moment decreases with increasing the number of neighboring Te atoms around the Cr atom and decreasing Cr-Te bond length. More neighboring S atoms and shorter Cr-Te bond length would induce stronger quenching of local magnetic moment of Cr atom due to the enhanced hybridization between Cr and Te atoms. It can be confirmed by the fact that there are 1, 2, 2, and 3 neighboring Te atoms for the isomers A4, A5, A3, and A1, respectively. The Cr-Te bond lengths for isomer A5 are larger than these of isomer A3, which

make local magnetic moment of isomer A5 larger than that of isomer A3 although they have the same neighboring Te atoms. We should point out that isomer A2 seems more particular, since Cr atom locates in the center of $(\text{ZnTe})_{12}$ cage with 12 neighboring Te atoms, and it has larger Cr-Te distance than the other four isomers.

We further explore the effect of Cr doping on the partial density of states (PDOS) for the most stable configuration A1 and metastable isomers A2 and A5. The PDOSs of substitutional isomer A1, endohedral isomer A2, and exohedral isomer A5 are shown in Figs. 2(a), (b), and (c), respectively. Gaussian broadening has been used while plotting the PDOS curves. It is found that for all the isomers, additional peaks contributed by Cr-3d states appear in the HOMO-LUMO gap of the host cluster. It is clear to see the hybridization between the Cr-3d and the nearest neighboring Te-5p for A1 and A5. While for A2, the Cr-3d state is more localized, which may account for the reason why the local magnetic moment of Cr atom is 5.58 near to the magnetic moment of an isolated Cr atom ($6\mu_B$).

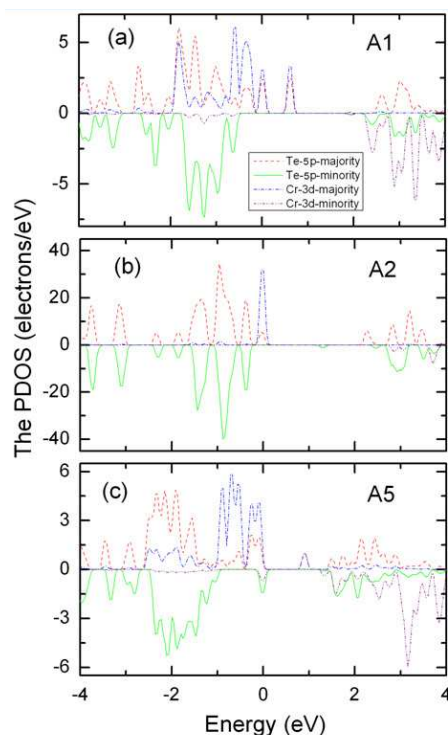


Figure 2: The PDOS of (a) isomer A1, (b) isomer A2, and (c) isomer A5.

3.3 Bidoped $(\text{ZnTe})_{12}$ clusters

In this section, we focus on the bidoped $(\text{ZnTe})_{12}$ clusters due to its magnetic coupling between the two Cr atoms. Bidoped isomers, including substitutional, exohedral, and endohedral doped clusters, are constructed from the monodoped $(\text{ZnTe})_{12}$ clusters, which will be

discussed in the following subsections.

3.3.1 Substitutional bidoped (ZnTe)₁₂ clusters

Due to high symmetry of the pristine (ZnTe)₁₂ cage, only five atomic configurations can be constructed for substitutional bidoped (ZnTe)₁₂ clusters. The fully optimized structures are shown in Fig. 1(b), labeled from B1 to B5 in order of increasing Cr-Cr distance. The geometrical structures of these clusters are somewhat distorted. Especially for B2 and B3, the geometrical structures are significantly distorted. In Table 2, we summarized the calculated results. The total magnetic moment of the FM state is $8\mu_B$ for all isomers, which mainly originates from Cr-3d states. Mulliken population analysis shows that the magnetic moment of the nearest neighboring Te atoms is antiparallel to that of the Cr atoms, indicating AFM coupling between them in all substitutional isomers.

Table 2: The distance of two Cr atoms (d_{Cr} , in Å), binding energy (E_b , in eV/atom), and HOMO-LUMO gap (in eV) of substitutional bidoped (ZnTe)₁₂ clusters. The local charge (Q_{Cr} , in a.u.), magnetic moment (μ_{Cr} , in μ_B) of Cr atoms and magnetic moment (μ_{Te} , in μ_B) of the nearest neighboring Te atoms in these clusters are also shown.

Isomers	FM						AFM					
	d_{Cr}	E_b	Gap	Q_{Cr}	μ_{Cr}	μ_{Te}	d_{Cr}	E_b	Gap	Q_{Cr}	μ_{Cr}	μ_{Te}
B1	3.01	-2.269	0.56	0.28	4.32	-0.77	3.07	-2.265	0.85	0.27	4.10	0
B2	3.82	-2.267	0.69	0.28	4.27	-0.69	3.03	-2.268	0.65	0.20	4.11	0.13
B3	6.07	-2.264	0.89	0.27	4.27	-0.34	6.06	-2.264	0.97	0.27	4.26	-0.36
B4	6.39	-2.262	0.59	0.30	4.28	-0.71	6.36	-2.262	0.83	0.30	4.26	0
B5	7.15	-2.262	0.67	0.30	4.27	-0.29	7.12	-2.262	0.84	0.30	4.27	0

For isomers B3, B4, and B5 with a large distance over 6 Å, the AFM and FM states are degenerate in energy, and have the same geometry, local charge, and magnetic moment except that the AFM state has a slightly larger HOMO-LUMO gap. The result means that magnetic coupling between the two Cr atoms is short-ranged. For isomer B1, the FM state is 0.004 eV/atom lower in energy than the AFM state, indicating the FM coupling via Te atoms are dominant over direct Cr-Cr AFM interaction. While for isomer B2, the AFM state is 0.003 eV/atom lower in energy than the FM state. The results indicate that direct Cr-Cr AFM interaction and the FM coupling via Te atoms are in competition. The structure of the AFM state of isomer B2 is somewhat distorted and the distance between the two Cr atoms become smaller than that of the AFM state of isomer B1, which make it more stable than that of isomer B1.

3.3.2 Exohedral bidoped (ZnTe)₁₂ clusters

We obtain five isomers for exohedral bidoped (ZnTe)₁₂ clusters as shown in Fig. 1(c), labeled from C1 to C5 in order of increasing Cr-Cr distance. The calculated results are listed in Table 3. The total magnetic moment of the FM state of the clusters is $8\mu_B$, independent of their atomic configuration. Similar to the case of substitutional bidoped isomers, the magnetic moment

arises mainly from the Cr-3d states. Mulliken population analysis shows that the magnetic moments of the nearest neighboring Te and Zn atoms are all antiparallel to that of the Cr atoms, indicating AFM coupling between them.

Table 3: The distance of two Cr atoms (d_{Cr} , in Å), binding energy (E_b , in eV/atom), and HOMO-LUMO gap (in eV) of exohedral bidoped (ZnTe)₁₂ clusters. The local charge (Q_{Cr} , in a.u.), magnetic moment (μ_{Cr} , in μ_B) of Cr atoms, and magnetic moment (μ_{Te} and μ_{Zn} , in μ_B) of the nearest neighboring Te atoms and Zn atoms in these clusters are also shown.

Isomers	FM							AFM						
	d_{Cr}	E_b	Gap	Q_{Cr}	μ_{Zn}	μ_{Te}	μ_{Cr}	d_{Cr}	E_b	Gap	Q_{Cr}	μ_{Zn}	μ_{Te}	μ_{Cr}
C1	3.11	-2.088	0.49	0.21	-0.18	-0.56	4.42	2.55	-2.125	0.61	0.13	0	0.06	4.31
C2	4.20	-2.116	0.96	0.09	-0.29	-0.30	4.32	3.96	-2.117	0.92	0.08	0.02	-0.11	4.27
C3	4.96	-2.132	0.94	0.11	-0.24	-0.34	4.33	4.94	-2.133	1.18	0.12	0.03	-0.08	4.36
C4	9.12	-2.083	0.83	0.19	-0.30	-0.32	4.35	9.12	-2.083	0.85	0.19	0	0	4.35
C5	9.29	-2.077	0.80	0.18	-0.31	-0.30	4.34	9.29	-2.077	0.86	0.19	0	0	4.36

As in the case of substitutional bidoped, isomers C4 and C5 with the Cr-Cr distance over 6 Å, the AFM state and the corresponding FM state are nearly degenerate with the same geometry, local charge, and magnetic moment. For isomers C1, C2, and C3 with a small Cr-Cr distance, the AFM state is more stable than the FM state. The relatively short Cr-Cr distance results in a strong AFM magnetic coupling in isomer C1 and C2, but isomers C3 is more favorable in energy than isomer C1. This is quite different from the substitutional bidoped isomers, in which the cluster cohesion sensitively depends on the magnetic coupling between Cr atoms. From Fig. 1(c), we can see that two Cr atoms in isomer C3 connect with the neighboring Te and Zn atoms, which forming additional four-member and six-member rings. Therefore, we conclude that the cluster cohesion for exohedral doping is sensitive to the chemical bonding. The ordering in binding energy is C3>C1>C2>C4>C5.

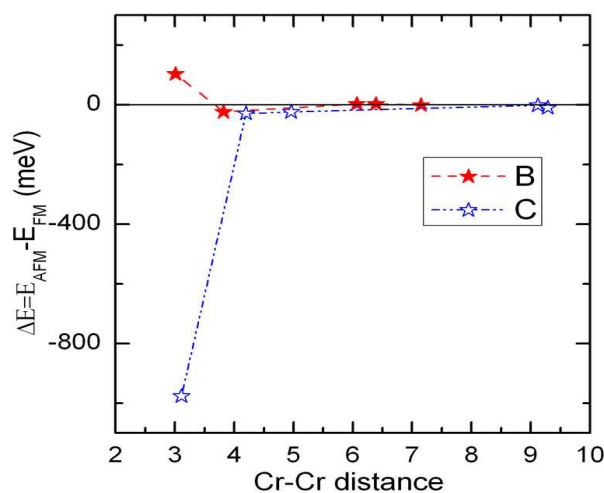


Figure 3: Energy difference between AFM and FM states for substitutional and exohedral bidoped isomers with respect to the Cr-Cr distance.

In Fig. 3 we show the variation of energy difference between the FM and AFM state of substitutional and exohedral bidoped isomers ($\Delta E = E_{AFM} - E_{FM}$) with respect to the Cr-Cr separation in FM states. The result clearly indicates that the nature of the coupling is short-ranged, a little larger than Zn-Te bond.

3.3.3 Endohedral bidoped (ZnTe)₁₂ clusters

The optimized geometry of endohedral bidoped (ZnTe)₁₂ clusters are shown in Fig. 1(d) (labeled as D-FM and D-AFM). The calculated results are summarized in Table 4. Compared with pristine (ZnTe)₁₂ cage, the endohedral bidoped (ZnTe)₁₂ are significantly distorted. Especially for the FM isomer, the two Cr atoms move close to the two six-member rings, which make the isomer distorted very much. The binding energies are significantly enhanced compared with the substitutional and exohedral bidoped isomers. The Cr-Cr distance of the AFM state (2.38 Å) is the smallest compared to all other bidoped isomers. The AFM state is 0.006 eV/atom lower than the FM state, which is the largest energy difference among all other bidoped isomers. We can conclude that the direct Cr-Cr AFM interaction is the strongest when encapsulated inside (ZnTe)₁₂ cluster, which makes the cluster be in favor of AFM state. Similar behavior was observed for the Cr-doped (CdS)₁₂ cage [16]. Furthermore, the AFM state has the largest HOMO-LUMO gap among all bidoped cases. The vibrational frequency is calculated for both FM and AFM states and no imaginary frequency is found for both of them, indicating that they are all stable around their local equilibrium structures. We further examine the stability of the AFM isomer by considering two fragmentation processes which include "the endohedral bidoped cluster \rightarrow (ZnTe)₁₂ + two isolated Cr atoms or a Cr₂ dimer." The obtained fragmentation energies are 4.15 and 2.90 eV, respectively. This indicates that the hollow cavity of the (ZnTe)₁₂ cage can hold the two Cr atoms steadily.

Table 4: The distance of two Cr atoms (d_{Cr} , in Å), binding energy (E_b , in eV/atom), HOMO-LUMO gap (in eV), and total magnetic moment (μ_{tot} , in μ_B) of endohedral bidoped (ZnTe)₁₂ clusters. The local charge (Q_{Cr} , in a.u.) and magnetic moment (μ_{Cr} , in μ_B) of Cr atoms, and magnetic moment (μ_{Te} and μ_{Zn} , in μ_B) of the Te atoms and Zn atoms in the cluster are also shown.

<i>D</i>	d_{Cr}	E_b	<i>Gap</i>	Q_{Cr}	μ_{Zn}	μ_{Te}	μ_{tot}	4s	4p	μ_{Cr} 3d	<i>total</i>
FM	3.01	-2.139	1.20	0.02 -0.02	0.17	0.19	10	0.18	0.19	4.44	4.81
AFM	2.38	-2.145	1.63	-0.08	0	0	0	20	0.13	4.18	4.51

3.3.4 Comparison between the most stable isomers of bidoped (ZnTe)₁₂ clusters

It is interesting to compare the bidoped clusters with different doping modes. Firstly, the relative stability of the bidoped clusters should be clarified. We will focus on the most energetically favorable configurations in the substitutional, exohedral, and endohedral bidoped clusters, i.e., the FM state of isomers B1 and the AFM state of isomers C3 and D. The vibrational properties of both C3 and B1 are calculated. From our calculations, no imaginary

frequency is found for both of them, indicating that they are all stable around their local equilibrium structures. It is noted that the isomers C3 and D have the same chemical composition. As shown in Tables 3 and 4, the binding energy of isomer C3 is 0.012 eV/atom higher than that of isomer D. This implies that isomer C3 would transform into other stable configurations if it deviates from its equilibrium structure too much, even though it behaves as a stable local minimum. Furthermore, the calculated fragmentation energy is about 1.312 eV for the fragmentation channel $D \rightarrow B1+2Zn$, indicating that the endohedral isomer is most favorable for bidoped clusters.

The PDOS of FM and AFM states of isomer B1, C3, and D are shown in Figs. 4(a-c) and (d-f). The spin-majority and spin-minority states are identical for the AFM states of B1 and D, consistent with its AFM nature. Although some polarized characteristics are observed near the Fermi level, there is no net magnetic moment for AFM state of C3. From Figs. 4(a) and (d), we can see that the contribution of $p-d$ hybridization width for FM state at Fermi level is larger compared to that of AFM state, which means that the $p-d$ hybridization is dominate for isomer B1.

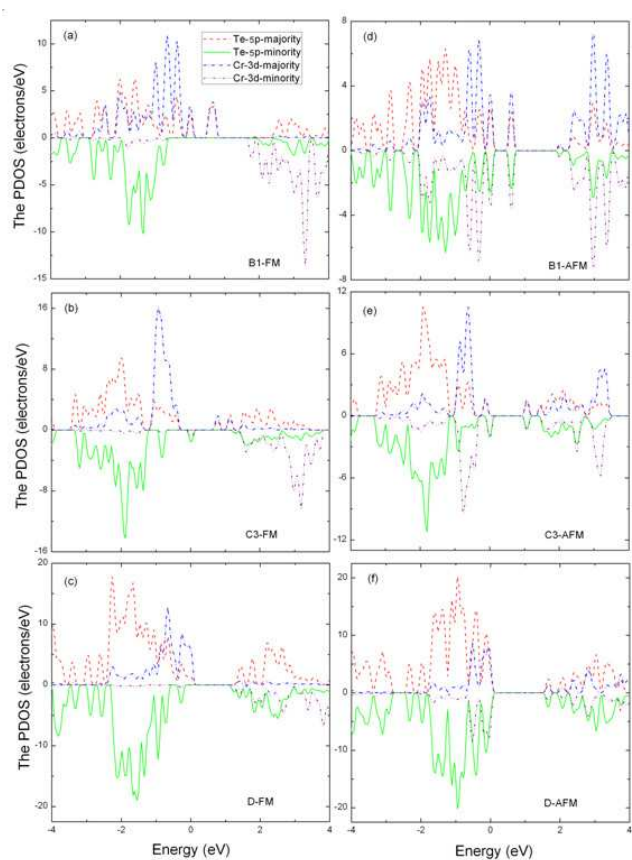


Figure 4: The PDOS of FM states (a-c) and AFM states (d-f) of isomer B1, C3, and D.

4 Conclusion

In conclusion, the structural, electronic, and magnetic properties of $(\text{ZnTe})_{12}$ clusters doped with Cr atoms have been studied by employing a first-principles method. For the monodoped case, we find the exohedral isomer is the most energetically favorable state. The magnetic moment of the monodoped clusters is dependent on the local environment of the Cr atom. For the bidoped cases, the endohedral isomers are found to be most favorable. The magnetic coupling between the Cr atoms in bidoped configurations is mainly governed by the competition between direct Cr-Cr AFM interaction and the FM interaction between two Cr atoms via Te atom due to strong p - d hybridization.

Acknowledgments. This work is supported by the Natural Science Foundation of Yancheng Teachers University under Grant No. 09YCKL007.

References

- [1] H. Ohno, *Science* 281 (1998) R29.
- [2] H. Saito, V. Zayets, S. Yamagata, and K. Ando, *Phys. Rev. Lett.* 90 (2003) 207202.
- [3] T. M. Pekarek, J. E. Luning, I. Miotkowski, and B. C. Crooker, *Phys. Rev. B* 50 (1994) 16914.
- [4] K. Sato and H. Katayama-Yoshida, *Semicond. Sci. Technol.* 17 (2002) 367.
- [5] Y. Xia, P. D. Yang, Y. G. Sun, *et al.*, *Adv. Mater.* 15 (2003) 353.
- [6] H. Yu, J. Li, R. A. Loomis, *et al.*, *Nature Mater.* 2 (2003) 517.
- [7] J. D. Holmes, K. P. Johnston, C. Doty, and B. A. Korgel, *Science* 287 (2000) 1471.
- [8] D. J. Norris, A. Lfros, and S. C. Erwin, *Science* 319 (2008) 1776.
- [9] D. V. Talapin and C. B. Murray, *Science* 310 (2005) 86.
- [10] M. Shim and P. Guyot-Sionnest, *Nature* 407 (2000) 981.
- [11] D. Yu, C. J. Wang, and P. Guyot-Sionnest, *Science* 300 (2003) 1277.
- [12] J. M. Matxain, J. M. Mercero, J. E. Fowler, and J. M. Ugalde, *Phys. Rev. A* 64 (2001) 053201.
- [13] J. M. Matxain, J. M. Mercero, J. E. Fowler, and J. M. Ugalde, *J. Am. Chem. Soc.* 125 (2003) 9494.
- [14] H. T. Liu, S. Y. Wang, G. Zhou, *et al.*, *J. Chem. Phys.* 124 (2006) 174705.
- [15] J. G. Wang, L. Ma, J. J. Zhao, *et al.*, *J. Chem. Phys.* 129 (2008) 044908.
- [16] S. Ghosh, B. Sanyal, and G. P. Das, *J. Magn. Magn. Mater.* 322 (2010) 734.
- [17] M. K. Yadav, B. Sanyal, and A. Mookerjee, *J. Magn. Magn. Mater.* 321 (2009) 235.
- [18] J. P. Perdew, K. Burke, and M. Ernzerhof, *Phys. Rev. Lett.* 77 (1996) 3865.
- [19] R. S. Mulliken, *J. Chem. Phys.* 23 (1955) 1841.
- [20] Y. Z. Liu, K. M. Deng, Y. B. Yuan, *et al.*, *Chem. Phys. Lett.* 469 (2009) 321.
- [21] C. X. Su and P. B. Armentrout, *J. Chem. Phys.* 99 (1993) 6506.